PCCP

ROYAL SOCIETY OF CHEMISTRY

PAPER

View Article Online
View Journal | View Issue

Cite this: *Phys. Chem. Chem. Phys.*, 2021, **23**, 21913

Probing the influence of Zn and water on solvation and dynamics in ethaline and reline deep eutectic solvents by ^{1}H nuclear magnetic resonance†

Yasmeen M. AlZahrani and Melanie M. Britton *

A range of ethaline and reline deep eutectic solvents (DESs) have been investigated in the absence and presence of Zn (0–0.3 M) and water (0–29 wt%) by one-dimensional ^{1}H NMR spectroscopy, two-dimensional ^{1}H–^{1}H nuclear Overhauser effect and exchange spectroscopy, ^{1}H T_1 NMR relaxation times and ^{1}H NMR diffusion. The role of zinc and water in controlling solvation and microstructure in reline and ethaline were investigated. We show that in ethaline there is proton exchange between hydroxyl groups in ethaline glycol and choline chloride. The rate of exchange between these protons is found to significantly increase in the presence of Zn, but decreases with increasing water content. In the case of reline, no proton exchange is observed between the amide protons in urea and hydroxyl protons in choline chloride. However, the addition of water decreases the viscosity of the system, as well as changes the distance between amide and hydroxyl protons in urea and choline chloride, respectively. The addition of Zn does not appear to change the interactions between urea and choline chloride species, but does reduce the rate of exchange between water and hydroxyl protons in reline formulations containing water.

Received 14th July 2021,
Accepted 15th September 2021

DOI: 10.1039/d1cp03204f

rsc.li/pccp

Introduction

In recent years, there has been increasing interest in the use of deep eutectic solvents (DESs) as a replacement for aqueous and organic electrolytes in many electrochemical applications, including metal electrodeposition,[1–3] metal electropolishing[4,5] and batteries.[6] This increasing interest largely arises from their high chemical stability, wide potential window, low flammability and volatility. Another important benefit of DESs is that they can be formed by mixing, typically, inexpensive, low-toxicity, biodegradable components, and, hence, also offer economic and environmental benefits.[7–9]

A widely investigated class of DES is based on the quaternary ammonium salt choline chloride (ChCl).[6,10,11] This class includes ethaline, which is a mixture of 1 : 2 molar ratio of ChCl and ethylene glycol (EG), and reline, a 1 : 2 molar ratio mixture of ChCl and urea (U).[12] While multiple interactions contribute to the intermolecular network within DESs, including van der Waals interactions, hydrogen bonding and/or ionic bonding,[13] it is hydrogen bonding that is considered to be the primary cause of their melting point depression and physicochemical properties, such as viscosity and conductivity.[8] Ethaline and reline have been investigated as more sustainable electrolytes in the electrodeposition of Zn, as an anti-corrosion layer.[3,11,14,15] However, zinc deposits have been found to have different morphologies, depending on the DES used, which has been attributed to differences in the hydrogen bond network between ethaline and reline systems[15] and zinc ion species, which play an important role in the mechanisms of deposition.[3] Abbott *et al.*[15] proposed that the predominant zinc species in both ethaline and reline systems is $[ZnCl_4]^{2-}$. Reline has also been investigated as a novel electrolyte for rechargeable zinc-batteries.[6] Reversible plating/stripping of zinc species has been observed, without hydrogen evolution or the formation of a passivation layer on the zinc electrode.[6] However, despite this initial interest in these DES systems for Zn-electrochemical applications, there are several challenges currently preventing their commercialisation. Primarily, these are associated with poor physical properties, such as their typically high viscosity, and, hence, lower conductivity.[12] Also, a lack of understanding of the species formed has limited the optimisation of DES formulations.[16]

In order to overcome poor physical properties in DESs, the addition of water has been investigated.[12,17–20] Computer simulations have revealed that the addition of water, to

School of Chemistry, University of Birmingham, Edgbaston, B15 2TT, UK.
E-mail: m.m.britton@bham.ac.uk

† Electronic supplementary information (ESI) available. See DOI: 10.1039/d1cp03204f

ethaline or reline DESs, decreases the number of hydrogen bonds formed and consequently lowers the viscosity of both DES systems.[20] However, as more water is added, it has been observed[12] that ChCl-based DESs start to lose their DES structure, and form aqueous solutions, above a 1 : 1 equivalent of water:-chloride. This transition is also reported to change the electrochemical properties of ChCl-based DESs, in particular, by narrowing their potential window.[21,22] Cyclic voltammetry (CV) experiments have shown that reline retains a wide potential window until the amount of added water reaches 9 wt%.[21] The effects of adding water to reline[21] and ethaline,[22] for electroplating Cu[22] and Ni[21] have been investigated. It has been observed that the addition of 15 wt% water in ethaline, for Cu electroplating, results in a reduction in the ethaline viscosity without reducing the wide potential of the electolyte.[22] Adding 6 wt% of water to reline, for nickel electroplating, lowers the reline viscosity, and suppresses nickel dendritic growth, resulting in a smooth, dense nickel deposit.[21]

The study of speciation and solvation, and the effect of additives such as water, on the chemical and physical properties of DES have been investigated computationally, using quantum mechanics (QM) simulations,[18,23] and experimentally, using nuclear magnetic resonance (NMR),[24] Fourier-transform infra-red (FTIR) and Raman spectroscopies.[25] In these studies, it has been proposed that the addition of water affects the hydrogen bond network of DESs, by forming new hydrogen bonds between water and DESs components, which subsequently affect the properties of the DES, such as viscosity.[18,23] Moreover, it has been observed that the number of hydrogen bonds formed between water and EG, in ethaline, are comparatively higher than those formed between water and U in the reline system.[25] In the case of reline, while water can hydrogen bond with ChCl and U,[19,23] it has been found that water molecules also occupy the interstices within the hydrogen bond network, reducing the number of hydrogen bonds between water and ChCl or U.[25] Following investigation by diffusion NMR, D'Agostino *et al.*[12] proposed that, in the presence of 20 wt% of water, ethaline forms a homogenous ethaline–water mixture, while reline forms a non-homogeneous reline–water mixture with a rich-water region. Zinc speciation in ethaline and reline has been studied using mass spectrometry.[26] However, as this is typically an *ex situ* technique, it is not able to provide information on speciation during electrochemical processes. Non-invasive, *in situ* techniques have been explored, which are able to provide information on speciation and dynamics of metal ions in DES electrolytes.[26] Furthermore, there is growing interest in developing operando techniques for observing speciation and dynamics, *in situ* and in real time, under working conditions. Such techniques have been demonstrated using ^{1}H NMR T_1 relaxation times to determine Zn speciation in aqueous electrolytes during Zn corrosion and discharging of a Zn-battery.[27,28]

In this paper, a range of ethaline and reline DESs have been investigated, in the absence and presence of Zn (0–0.3 M) and water (0–29 wt%). Molecular interactions and dynamics have been investigated using one-dimensional (1D) ^{1}H NMR and two-dimensional (2D) ^{1}H–^{1}H nuclear Overhauser exchange (NOESY) and exchange (EXSY) NMR spectroscopy. The influence of zinc and water, on the mobility and microstructure with each DES system, has been investigated using ^{1}H NMR T_1 relaxation time and diffusion measurements. We demonstrate that the zinc species are different in ethaline and reline, and the interaction between zinc and water is also different in ethaline and reline.

Experimental details

Materials and samples preparation

Choline chloride (ChCl, 99%), ethylene glycol (EG, 99.8%), urea (U, 99.9%) and zinc chloride ($ZnCl_2$, 99.99%) were supplied by Sigma-Aldrich. All components were used without further purification, but dried in a vacuum oven under reduced pressure (100 mbar), at 80 °C (ChCl, EG and U) or at 120 °C ($ZnCl_2$), for a minimum of 24 hours and were stored in a glove-box under argon atmosphere. In a glove-box, ethaline was prepared by mixing ChCl and EG in a 1 : 2 molar ratio and reline was prepared by mixing ChCl and U in a 1 : 2 molar ratio before sonication and heating to 60 °C until homogenous clear colourless liquids were formed. Solutions of zinc in ethaline or reline were prepared in a glove-box by dissolving dry $ZnCl_2$ in either ethaline or reline, over a range of $ZnCl_2$ concentrations (0.1, 0.2 and 0.3 M in ethaline and 0.3 M in reline) at 25 °C. A range of concentrations of water were prepared by adding water (Nanopure filtered, resistivity 18 MΩ cm), to ethaline and reline, in the presence and absence of 0.3 M $ZnCl_2$. Solutions of water in ethaline, at concentrations of 2.7, 5.5, 8.3, 16 and 29.2 wt%, were prepared by adding 26, 52, 79, 151 and 277 μl, respectively, of water to 850 μl of ethaline. Solutions of water in reline, at concentrations of 5.5, 8.3 and 26.2 wt%, were prepared by adding by adding 58.5, 88 and 279 μl of water, respectively, to 850 μl of reline. Samples were put, immediately after preparation, into 5 mm Wilmad® NMR tubes fitted with J Young valves, to prevent the absorption of additional water. NMR measurements were performed <12 h after sample preparation. The amount of water in each sample was confirmed using ^{1}H NMR spectroscopy.

NMR measurements

NMR data were collected on a Bruker AVANCE III HD 300 spectrometer equipped with a 7 T vertical wide-bore superconducting magnet, operating at a proton resonance frequency of 300.13 MHz, with a 10 mm ^{1}H diff30 radiofrequency (RF) coil. NMR experiments were performed at 293 ± 0.3 K, controlled by the temperature of the water-cooled gradient coils. The 90° RF pulse was calibrated for each sample and found to be 20 ± 1 μs.

^{1}H NMR spectra were acquired using a pulse-acquire sequence, with a repetition time of 6 s. The chemical shift of peaks were calibrated to an external reference of TMS in deuterated chloroform, which was put in a 10 mm NMR tube, with the sample in a 5 mm NMR tube inside. 2D ^{1}H–^{1}H NOESY experiments were acquired using the sequence, $[90^\circ - \tau_1 - 90^\circ - \tau_{mix} - 90^\circ - acq]$, with 256 point in the F1 direction and 2048 in the F2 direction, with a repetition time of 2 s, 16 signal

averages and 16 dummy scans. The mixing time, τ_{mix}, was increased from 0 to 300 ms, over a series of six experiments. Proton exchange rates (k_{ex}) were calculated,[29] by fitting, in Kaleidagraph,[30] the signal intensity of exchange peaks (I_{AB} and I_{BA}), as a function of mixing time (τ_{mix}), to eqn (1):

$$I_{AB} = I_{BA} = P_A P_B(1 - \exp(-k_{ex}\tau_{mix}))\exp(-R_1\tau_{mix}) \quad (1)$$

where $P_A = \frac{I_A}{I_A + I_B}$, $P_B = \frac{I_B}{I_A + I_B}$ and $R_1 = (R_{1A} + R_{1B})$, I_A and I_B are the intensities at $\tau_{mix} = 0$ ms, and R_{1A}, R_{1B} are the relaxation rates of species A and B. In the fitting, an average value of I_{AB} and I_{BA} was used. Exchange peaks were identified as having the same phase as the diagonal peaks, which, in this study, are plotted positively. Cross-peaks arising from the nOe have a phase depending on the molecular size of species and viscosity of the solvent.[31] In the case of small molecules in low viscosity DES, where tumbling rates are faster, the nOe cross-peaks are expected to have the opposite sign to diagonal peaks and are negative where diagonal peaks are positive. For molecules in high viscosity solvents, where molecular tumbling is slow, the nOe cross-peaks are expected to be positive, where diagonal peaks are also positive.

Spin–lattice (T_1) NMR relaxation times were measured using an inversion recovery experiment,[31] $[180^\circ - \tau - 90^\circ - \text{acq}]_n$, with a repetition time of 6 s and 8 signal averages. A series of spectra ($n = 12$) were collected with logarithmically spaced time delays, τ, ranging from 5×10^{-6} s to 6 s. T_1 relaxation times were determined by fitting the normalised signal intensity ($I_{(\tau)}/I_{(0)}$), as a function of time, to eqn (3).

$$\frac{I(\tau)}{I(0)} = 1 - 2\exp^{\frac{-\tau}{T_1}} \quad (3)$$

Self-diffusion co-efficients (D) were measured using a pulsed gradient stimulated echo (PGSTE) sequence[31] with 16 gradient steps. Diffusion measurements of dry ethaline samples were collected with a maximum gradient (G_{max}) of 300 G cm^{-1}, pulse duration (δ) of 2 ms, observation time (Δ) of 60 ms, and repetition time of 2 s. Diffusion measurements of dry reline samples were collected using G_{max} = 600 G cm^{-1}, δ = 2 ms, Δ = 100 ms, with a repetition time of 2 s. Diffusion measurements for ethaline and reline systems containing water were collected using G_{max} = 300 G cm^{-1}, δ = 2 ms, Δ = 30 ms, and a repetition time of 4 s. The average self-diffusion co-efficients (D) were determined by fitting the normalised signal intensity as a function of gradient strength, ($I_{(G)}/I_{(0)}$), to the Stejskal–Tanner[32] eqn (4). Where a single diffusion co-efficient was not sufficient to fit the data, fitting to a bi-exponential function was performed.

$$\frac{I(G)}{I(0)} = \exp\left[-\gamma^2\delta^2G^2D\left(\Delta - \frac{\delta}{3}\right)\right] \quad (4)$$

Results

Fig. 1 shows the ^{1}H NMR spectra for dry ethaline and reline DESs, along with the molecular structures and proton labelling scheme of constituent species in each DES. The broad line widths

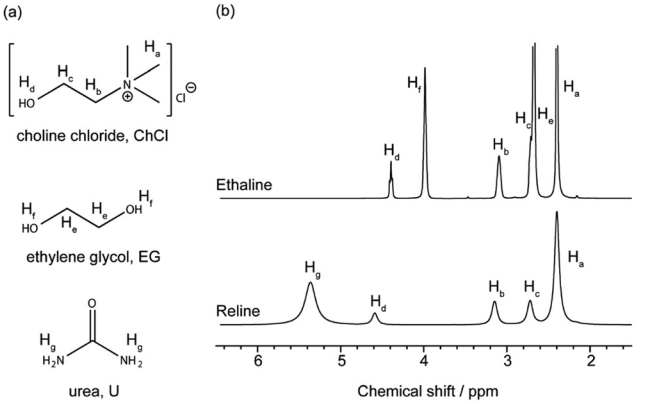

Fig. 1 (a) Molecular structures for the constituent species of ethaline (1ChCl:2EG) and reline (1ChCl:2U) with proton numbering scheme, and (b) ^{1}H NMR spectra for pure dry ethaline and reline systems, at 293 K.

observed for peaks in the ^{1}H NMR spectrum of reline are indicative of the higher viscosity for reline compared to ethaline.

^{1}H NMR spectra for dry ethaline and reline, with increasing $ZnCl_2$ concentration, are shown in Fig. 2. For both reline and ethaline, no visible change in viscosity was observed upon the addition of zinc. This observation is consistent with the ^{1}H NMR spectra in Fig. 2, which do not show a change in line width for the peaks of the non-exchanging protons (H_a, H_b, H_c and H_e; Table S1 in the ESI†). In the ethaline system, the line widths for hydroxyl protons in choline cation (Ch^+) and EG (H_d and H_f respectively) are observed to increase gradually, as the concentration of Zn increases. This is matched by a slight upfield shift of the peak for the hydroxyl proton in Ch^+ (H_d). However, in the reline system, the line width and chemical shift for the H_d peak do not appear to be affected by the addition of zinc.

Fig. 3 shows ^{1}H NMR spectra for ethaline, in the presence and absence of Zn and water. There is a gradual shift for all hydroxyl proton peaks (H_d, H_f and H_w) downfield, as the water content increases. Also, the addition of water narrows the line width for (H_a, H_b, H_c and H_e) peaks, irrespective of whether Zn is present or not. However, the presence of zinc broadens the H_d, H_f and H_w peaks.

Fig. 4 shows ^{1}H NMR spectra for reline, in the presence and absence of Zn and water. The presence of Zn does not appear to have a significant effect on the ^{1}H NMR spectra. However, the presence of water leads to a significant reduction in line width of the urea peak (H_g), which also shifts upfield as the water content increases. The water peak (H_w) shifts gradually to higher chemical shift, as water content increases. As the water content increases, both in the presence and absence of Zn, there is a slight reduction in the line width of the H_a, H_b, H_c and H_g peaks. The addition of water broadens, and slightly shifts down field, the peak for the hydroxyl protons in Ch^+ (H_d). At the highest water content, the H_d peak overlaps completely with H_w peak, in the absence of Zn (Fig. 4a), whereas in the presence of Zn (Fig. 4b), the H_d peak remains at 4.6 ppm. However, the presence of zinc affects the line width of H_d and H_w peaks, which become narrower in the presence of Zn.

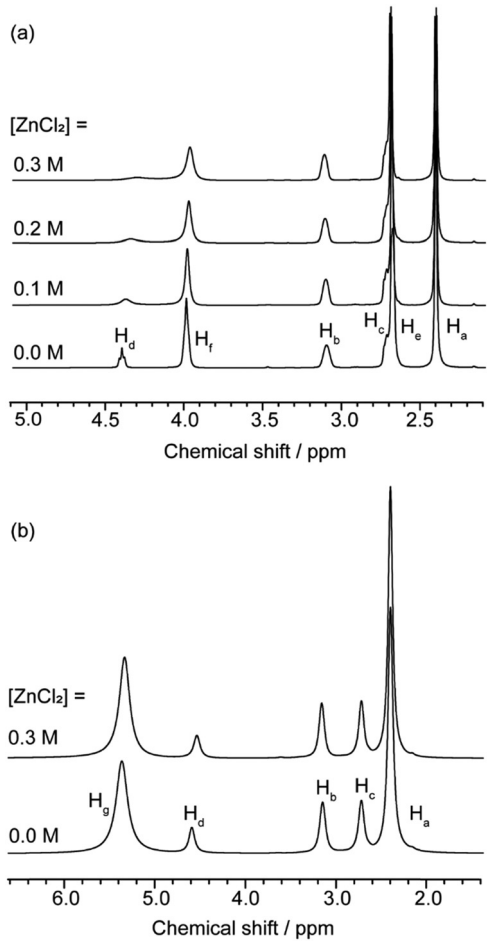

Fig. 2 A series of ^{1}H NMR spectra for dry (a) ethaline and (b) reline as a function of $ZnCl_2$ concentration, at 293 K. Molecular structures and numbering scheme of peak assignments were presented in Fig. 1. Associated line widths can be found in Table S1 in the ESI.†

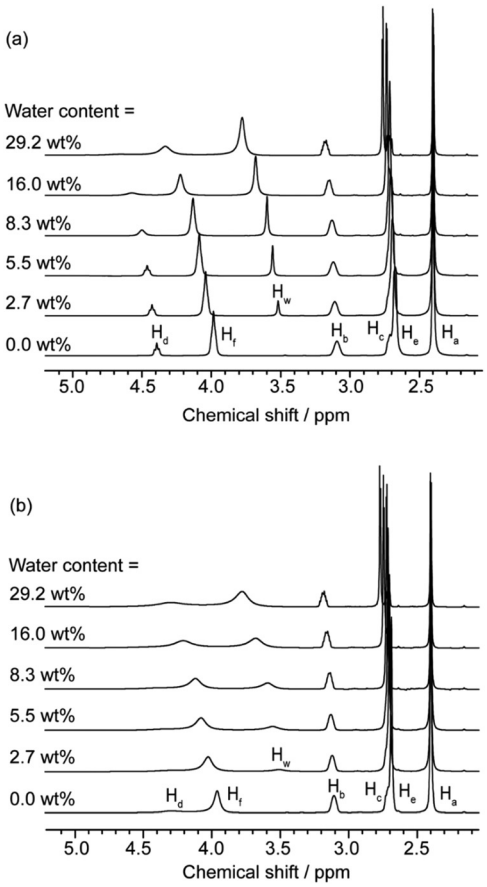

Fig. 3 A series of ^{1}H NMR spectra for ethaline system in the absence (a) and presence (b) of 0.3 M $ZnCl_2$ as a function of water content (H_w), at 293 K. Molecular structures and numbering scheme of peak assignments were presented in Fig. 1. Associated line widths can be found in Table S2 in the ESI.†

Fig. 5 shows 2D NOESY spectra for dry ethaline, in the presence and absence of $ZnCl_2$. In the absence of Zn, intense exchange (positive) peaks are observed between the hydroxyl protons (H_d and H_f) of Ch^+ and EG (Fig. 5a). The hydroxyl proton peaks, and exchange peaks, broaden in the presence of Zn (Fig. 5b), indicating increased exchange. 2D NOESY spectra for ethaline with 8.3 wt% water, in the presence and absence Zn, are shown in Fig. 6. Exchange peaks are observed between water (H_w) and the hydroxyl protons in Ch^+ and EG (H_d and H_f). In the presence of Zn, however, these exchange peaks are broader. In addition to the exchange peaks, nOe (negative) cross-peaks are also observed between the other protons in EG and Ch^+, which appear to become less intense in the presence of Zn.

Fig. 7–9 show 2D NOESY spectra for reline with 0, 8.3 and 26 wt% water, respectively, in the presence and absence of $ZnCl_2$. The higher viscosity of reline at 0 and 8.3 wt% water has led to all cross-peaks being positive.[33] In the dry reline system (Fig. 7), cross-peaks peaks are observed between the hydroxyl protons in Ch^+ (H_d) and the amide protons in U (H_g). However, as the viscosity of this system is high, it is not possible to identify whether these cross-peaks arise from exchange or nOe interactions. In the presence of water (Fig. 8), no cross-peaks are observed between these protons, indicating no exchange nor spatial proximity. The spectra in Fig. 8 show cross-peaks between H_g protons and the aliphatic protons in Ch^+ (H_a, H_b and H_c). These are negative and hence arise from the nOe, indicating their close spatial-proximity. Table 1 shows the proton exchange rates (k_{ex}), for both reline and ethaline, determined from the 2D ^{1}H–^{1}H NOESY spectra. Proton exchange is observed between the hydroxyl protons in Ch^+ (H_d) and water protons (H_w) in Fig. 8 and 9, as has been observed previously.[24] This exchange appears to increase with increasing water concentration (Fig. 4), resulting in a coalesced peak in the NOESY spectrum (Fig. 9) and a cross peak between $H_{d,w}$ and the amide protons H_g.

Diffusion co-efficients for Ch^+, in dry ethaline and reline, are shown in Table 2. It can be seen that, Ch^+ has a lower mobility in reline than ethaline, as expected because of the higher viscosity in reline. The diffusion coefficient for Ch^+ is largely unaffected by the presence of zinc. However, in ethaline, the diffusion co-efficient for the hydroxyl (H_d) and methyl protons (H_a), in Ch^+, are the same in the absence of Zn, but are different in the presence of Zn.

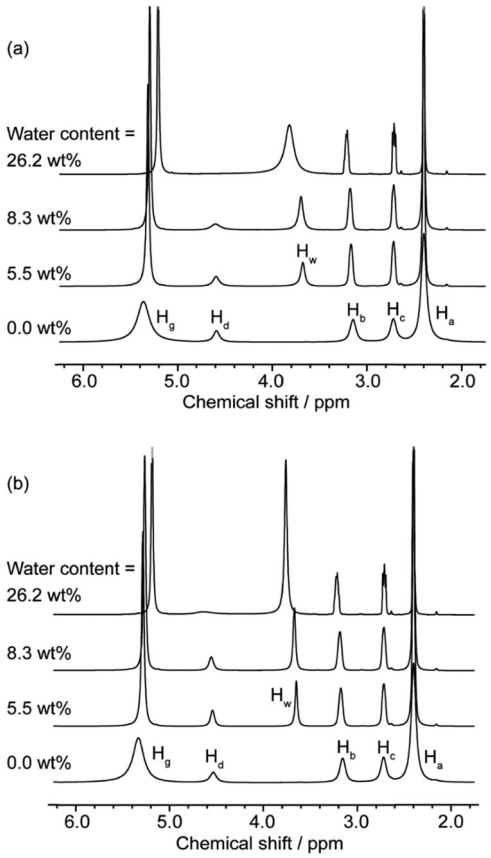

Fig. 4 A series of ^{1}H NMR spectra for reline system in the absence (a) and presence (b) of 0.3 M $ZnCl_2$ as a function of water content (H_w), at 293 K. Molecular structures and numbering scheme of peak assignments were presented in Fig. 1. Associated line widths can be found in Table S3 in the ESI.†

Diffusion co-efficients for ethaline species, with increasing water content, in the absence and presence of $ZnCl_2$, are presented in Tables 3 and 4, respectively. These data show that diffusion co-efficients, for all species, increase with increasing water content. At lower concentrations of water ($\leq$8.3 wt%), two diffusion co-efficients are observed for water. However, at high concentrations of water (29 wt%), only a single diffusion co-efficient is observed.

Diffusion co-efficients for Ch^+, U and water in reline, with increasing water content and in the absence and presence of $ZnCl_2$, are presented in Tables 5 and 6, respectively. It can be seen that the diffusion co-efficients of both Ch^+ and U increase with the addition of water, as expected. Two diffusion co-efficients are observed for water for all water concentrations. The diffusion co-efficients reported in our study are comparable with those reported by D'Agostino *et al.*[12] However, only a single diffusion coefficient was observed for water in their study.

Fig. 9 shows the T_1 relaxation times for Ch^+, in ethaline and reline, in the presence and absence of zinc and water. It can be seen that for ethaline, the T_1 NMR relaxation time for the H_a protons in Ch^+ increases, monotonically, with water content, but with a slight discontinuity around 8 wt% of water. However, for reline, the T_1 relaxation time for the H_a protons in Ch^+ decreases on addition of water, but then increases with increasing water content.

Discussion

The viscosity of ethaline is lower than the viscosity of reline, because U is a much stronger HBD than EG, therefore, reline is ten times more viscose than ethaline.[15] The effect of zinc on the viscosity of reline and ethaline has been studied previously.[15] It has been shown that the viscosity of ethaline is largely unaffected by the addition of Zn, but for reline, a significant decrease in viscosity was observed with increasing Zn.[15] The effect is expected to be minimised for ethaline because it already has a low viscosity ($\sim$22 cP for $[ZnCl_2]$ = 0 to 0.3 mol dm^{-3}), compared to reline ($\sim$800 cP to 280 cP for $[ZnCl_2]$ = 0 to 0.3 mol dm^{-3}).[15] However, the significant change in viscosity for reline, when Zn was added, was not observed in our study. This could be explained by our use of dried $ZnCl_2$,

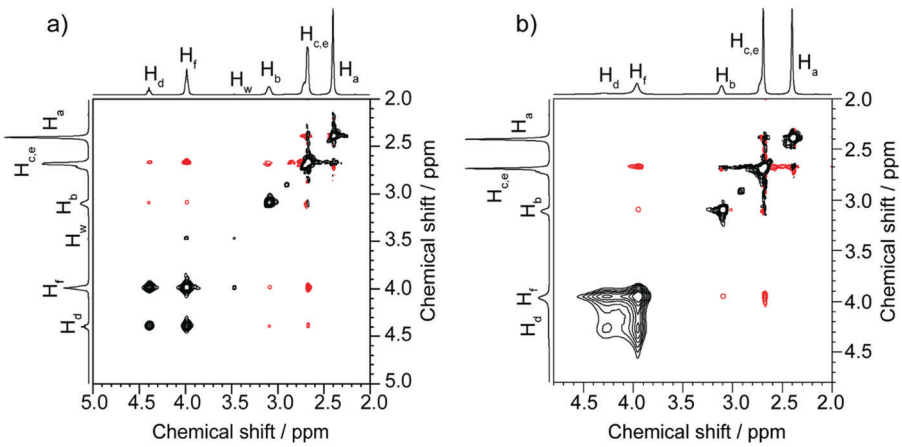

Fig. 5 ^{1}H–^{1}H NOESY NMR spectra for dry ethaline samples in the absence (a) and presence (b) of 0.3 M $ZnCl_2$, for a mixing time τ_m 300 ms. Positive peaks are black, negative peaks are red.

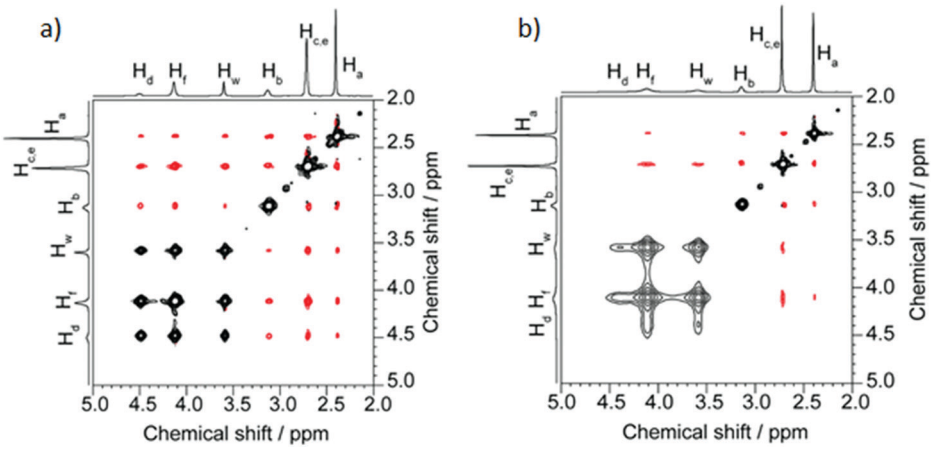

Fig. 6 $^{1}H-^{1}H$ NOESY NMR spectra for ethaline samples with addition of 8.3 wt% water in the absence (a) and presence (b) of 0.3 M $ZnCl_2$, for a mixing time τ_m 300 ms. Positive peaks are black, negative peaks are red.

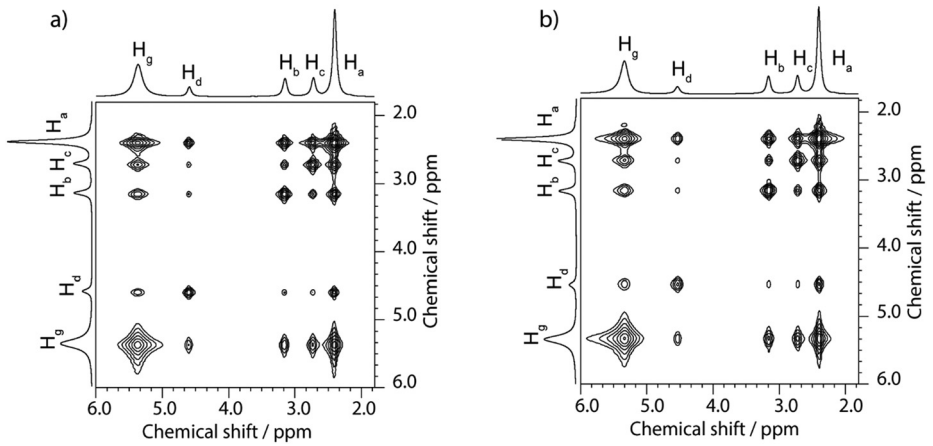

Fig. 7 $^{1}H-^{1}H$ NOESY NMR spectra for dry reline samples in the absence (a) and presence (b) of 0.3 M $ZnCl_2$, for a mixing time τ_m 100 ms. All peaks are positive (black) and no negative peaks (red) are observed.

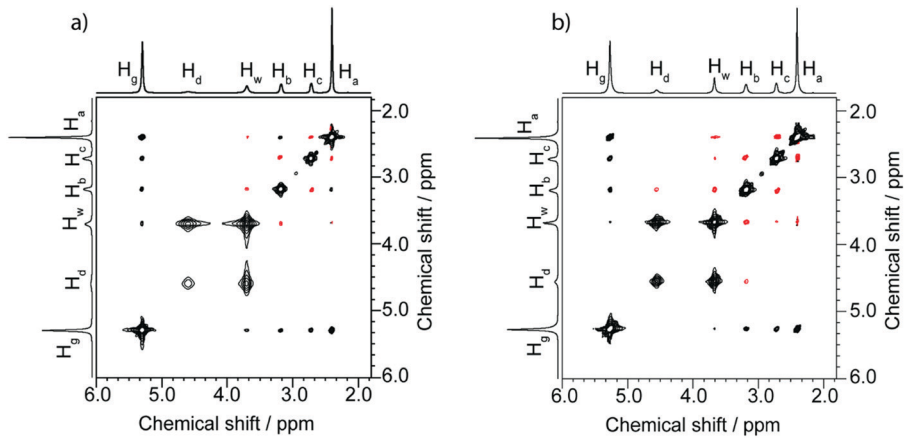

Fig. 8 $^{1}H-^{1}H$ NOESY NMR spectra for reline samples with addition of 8.3 wt% water in the absence (a) and presence (b) of 0.3 M $ZnCl_2$, for a mixing time τ_m 300 ms. Positive peaks are black, negative peaks are red.

Table 1 Proton exchange rates (k_{ex}) for ethaline and reline systems, at $[Zn^{2+}]$ = 0 and 0.3 M, at different water concentrations. Note, some exchange rates could not determine due to overlap of peaks, such as H_f–H_d for dry ethaline in presence of Zn. Also, an exchange rate between H_g–H_w protons could not be determined from the mixing times used in these experiments, where longer mixing times required

Water wt%	$[Zn^{2+}]$ = 0 M	$[Zn^{2+}]$ = 0.3 M
Ethaline		
0	k_{ex} (H_f–H_d) 11.36 s^{-1}	—
8.3	k_{ex} (H_f–H_d) 8.66 s^{-1} k_{ex} (H_w–H_f) 5.71 s^{-1} k_{ex} (H_w–H_d) 1.03 s^{-1}	k_{ex} ($H_{d,f}$–H_w) 77.8 s^{-1}
29	k_{ex} (H_f–H_d) 7.96 s^{-1} k_{ex} (H_w–H_f) 29.3 s^{-1} k_{ex} (H_w–H_d) 10.8 s^{-1}	k_{ex} ($H_{d,f}$–H_w) 124.8 s^{-1}
Reline		
8.3	k_{ex} (H_d–H_w) 77 s^{-1}	k_{ex} (H_d–H_w) 24 s^{-1}

compared to the previous study,[15] which used $ZnCl_2$ as obtained. As $ZnCl_2$ is hygroscopic, it is possible the previously observed change in viscosity could be due to the introduction of water. The possible effects of added water to the viscosity of ethaline are not observed, because of its significantly lower viscosity.

From previous studies of ethaline,[34] it is known that the hydroxyl groups of Ch^+ and EG coordinate around the Cl^-, bringing the H_d and H_f protons into close proximity. It is expected that this close proximity will facilitate proton exchange, which is observed in this study, by the presence of positive cross-peaks between H_d and H_f protons in the NOESY spectrum of pure ethaline (Fig. 5a). When water is added, it is known[17] that water also coordinates with the Cl^-, Ch^+ and EG. Again, this proximity is expected to facilitate exchange between H_d, H_f and H_w protons. This has been observed previously by diffusion NMR[12] and is also observed, in this study, by the positive cross-peaks between H_d, H_f and H_w protons in the NOESY spectrum (Fig. 6a). However, this study has shown, for the first time, that the addition of zinc, to both pure ethaline and ethaline-water systems, increases the rate of exchange between these protons (Table 1). This increase in proton exchange explains the increase in diffusion co-efficient for the H_d proton in the presence of Zn (Table 2). These observations indicate that EG, Ch^+ and water are predominantly co-ordinated around Zn^{2+}, rather than Cl^-.

Table 2 Diffusion co-efficients of Ch^+ alkyl protons (H_a) and Ch^+ hydroxyl protons (H_d) in dry ethaline and reline species in the absence and presence of $ZnCl_2$

	Diffusion co-efficient/10^{-11} m^2 s^{-1}	
System	H_a	H_d
Ethaline	1.92 ± 0.06	1.90 ± 0.07
Ethaline + 0.3 M $ZnCl_2$	1.76 ± 0.01	2.23 ± 0.07
Reline	0.05 ± 0.01	0.06 ± 0.01
Reline + 0.3 M $ZnCl_2$	0.06 ± 0.01	0.06 ± 0.01

Table 3 Diffusion co-efficients of ethaline species, Ch^+ (H_a) and EG (H_e), as a function of water (H_w) in the absence of zinc

	Diffusion co-efficient/10^{-11} m^2 s^{-1}, (contribution %)		
Water (wt%)	H_a	H_e	H_w
5.5	3.12 ± 0.01	5.46 ± 0.03	3.40 ± 0.08 (5.1 ± 0.1%) 15.47 ± 0.04 (94.9 ± 0.1%)
8.3	3.66 ± 0.01	6.33 ± 0.14	4.23 ± 0.01 (14.1 ± 1.1%) 16.25 ± 0.49 (85.9 ± 1.1%)
29.2	8.91 ± 0.07	14.61 ± 1.00	30.75 ± 0.46

Table 4 Diffusion co-efficients of ethaline species, Ch^+ (H_a) and EG (H_e), as a function of water (H_w) in the presence of 0.3 M $ZnCl_2$

	Diffusion co-efficient/10^{-11} m^2 s^{-1}, (contribution %)		
Water wt%	H_a	H_e	H_w
5.5	2.91 ± 0.03	5.19 ± 0.01	1.72 ± 0.23 (13.1 ± 3.4%) 14.22 ± 0.25 (86.9 ± 3.4%)
8.3	3.54 ± 0.06	6.34 ± 0.20	3.28 ± 0.49 (57.0 ± 23.7%) 12.75 ± 4.94 (43.0 ± 23.7%)
29.2	8.90 ± 0.45	16.24 ± 2.00	9.60 ± 0.71 (10.8 ± 2.6%) 31.75 ± 0.78 (89.2 ± 2.6%)

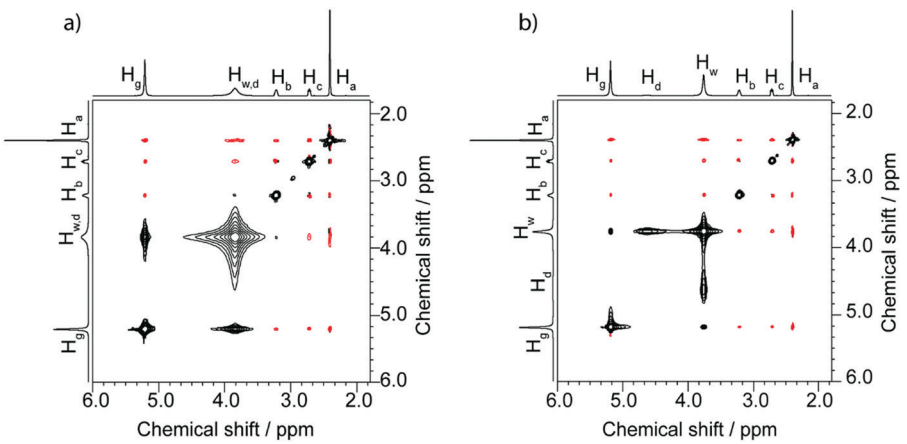

Fig. 9 ^1H–^1H NOESY NMR spectra for reline samples with addition of 26 wt% water in the absence (a) and presence (b) of 0.3 M $ZnCl_2$, for a mixing time τ_m 100 ms. Positive peaks are black, negative (nOe) peaks are red.

Table 5 Diffusion co-efficients of reline species, Ch^+ (H_a) and U (H_g) as a function of water (H_w) in the absence of zinc

	Diffusion co-efficient/10^{-11} m^2 s^{-1}, (contribution %)		
Water (wt%)	H_a	H_g	H_w
5.5	0.60 ± 0.04	1.02 ± 0.07	0.93 ± 0.06 (20.0 ± 1.2%) 4.57 ± 0.21 (80.0 ± 1.2%)
8.3	1.18 ± 0.15	1.98 ± 0.23	1.77 ± 0.13 (13.0 ± 1.1%) 7.83 ± 0.49 (87.0 ± 1.1%)
26.2	9.26 ± 0.45	14.33 ± 0.61	12.93 ± 0.04 (3.2 ± 0.5%) 38.06 ± 0.93 (96.8 ± 0.5%)

Table 6 Diffusion co-efficients of reline species, Ch^+ (H_a) and U (H_g) as a function of water (H_w) in the presence of 0.3 M $ZnCl_2$

	Diffusion co-efficient/10^{-11} m^2 s^{-1}, (contribution %)		
Water (wt%)	H_a	H_g	H_w
5.5	0.64 ± 0.03	1.12 ± 0.05	1.08 ± 0.12 (17.0 ± 0.4%) 5.99 ± 0.16 (83.0 ± 0.4%)
8.3	1.28 ± 0.09	2.19 ± 0.15	2.22 ± 0.10 (11.7 ± 0.4%) 9.64 ± 0.42 (88.3 ± 0.4%)
26.2	10.01 ± 0.25	15.67 ± 0.7	10.11 ± 0.06 (23.8 ± 1.6%) 32.85 ± 0.29 (76.2 ± 1.6%)

From previous studies of reline,[35] it has been suggested that the hydroxyl group in Ch^+ and carbonyl group in U co-ordinate around the Cl^- ion. It is expected that such an orientation reduces the opportunity for proton exchange between H_d (U) and H_g (Ch^+) protons. This is supported by the diffusion data (Table 2), which show that alkyl and hydroxyl protons in Ch^+ diffuse at the same rate. However, the 2D ^1H–^1H NOESY spectrum shows a cross peak between H_d and H_g protons (Fig. 7a). If proton exchange is not the origin of this cross peak, it can arise from the nOe, indicating these protons are in close ($\lesssim$3 Å) proximity. The addition of Zn does not appear to change the interactions between U and Ch^+ species, where 1D ^1H (Fig. 4) and 2D ^1H–^1H NOESY (Fig. 7) spectra and ^1H diffusion data (Table 2) are observed to remain largely unchanged.

When water is added to reline, it has been previously observed[23] that water coordinates with Cl^- and Ch^+. This co-ordination brings the H_w and H_d protons into close proximity, facilitating proton exchange between these protons. This is observed in this study in the 2D ^1H–^1H NOESY spectra (Fig. 8 and 9). In the NOESY spectrum with 8.3% wt water (Fig. 8a), not only is a cross peak observed between H_d and H_w protons, but there is now an absence of an nOe interaction between H_g and H_d protons, indicating a change in co-ordination between U and Ch^+ species. The addition of water to reline, in the presence of Zn, does not appear to change the interactions between U or Ch^+ species (Fig. 4 and 8) However, the presence of zinc appears to slow the exchange rate between H_d and H_w protons (Table 1). This is also supported by the 1D ^1H NMR spectra (Fig. 4b), where, in the presence of Zn, there is a narrowing of the line width of H_d and H_w peaks, which suggests that the presence of Zn slows down proton exchange. It is not clear why this is, but it could be because Zn^{2+} may compete with Cl^- to co-ordinate with either the water or Ch^+, or both, and thus reduces the number H_d and H_w protons able to exchange.

For both ethaline and reline, the addition of water reduces the viscosity.[12] This can be seen in the narrowing of peaks for non-exchangeable protons (Fig. 3 and 4) and increase in T_1 relaxation times (Fig. 10) and diffusion co-efficients, with increasing water (Tables 3–6). However, the T_1 relaxation time and diffusion co-efficient data also indicate a phase transition for both reline and ethaline with increasing water concentration. This can be seen in (Fig. 11), where these data are combined into a single plot for each DES. In ethaline, a discontinuity is observed in T_1 data around 8.3 wt% water. A more marked discontinuity in the T_1 relaxation time is observed for reline, where there is an initial decrease then increase. It should be noted, that a similar discontinuity can also be observed in the diffusion co-efficient data reported by D'Agostino *et al.*,[12] where a wider range of water concentrations were investigated. The origins of this behaviour in reline are most likely to come from a change in the distribution of water within the system. At low

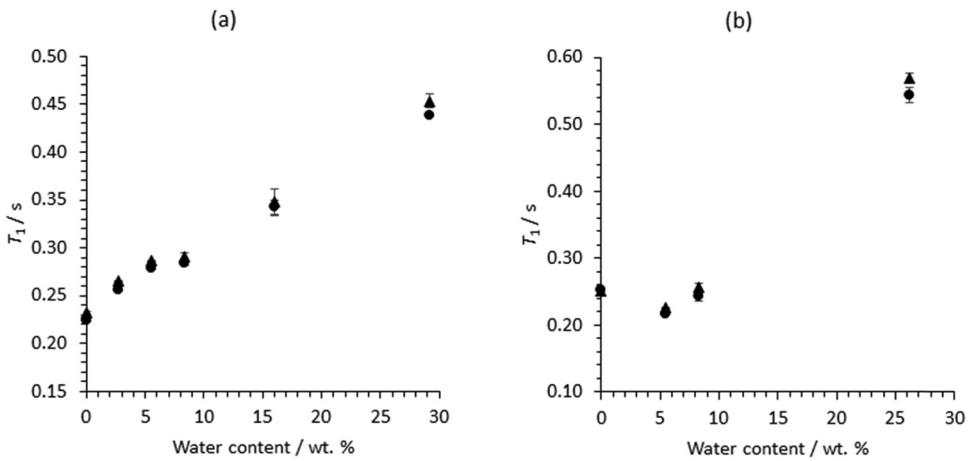

Fig. 10 T_1 relaxation times for Ch^+ protons (H_a), in (a) ethaline and (b) reline, as a function of water content, (●) in the absence and (▲) presence of 0.3 M $ZnCl_2$.

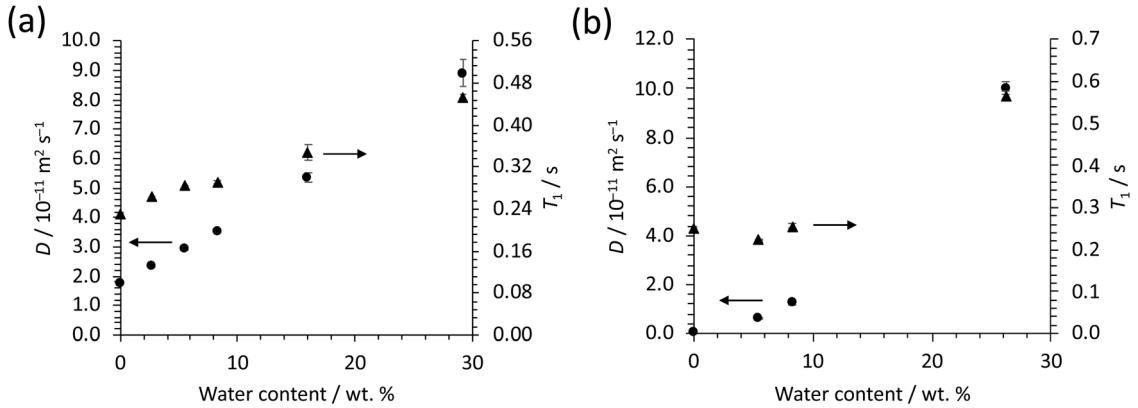

Fig. 11 Plot of T_1 relaxation times (▲) and diffusion co-efficient (●) for ChCl protons (H_a) in (a) ethaline and (b) reline, as a function of water content.

concentrations, water molecules embed in the reline network, forming a supermolecular complex. In such structures, there is an associated increase in size, leading to a higher rotational correlation time, for ChCl, and, hence, lower T_1 relaxation time.[36] However, when the water content increases (>6 wt%), there is an increase in the T_1 relaxation time for ChCl, which suggests a reduction in the tumbling rate for ChCl, indicating a change in the structures (solvation) formed within reline. This observation could be indicative of a transition to the heterogeneous distribution of water from discrete microscopic 'pockets' of water, within the reline network, proposed by Posada *et al.*[24] and D'Agostino *et al.*[12] at high water concentrations. Ethaline shows more of a monotonic increase in T_1 relaxation time, with increasing water content. However, a slight discontinuity can also be observed around 8 wt% of water, which is at a concentration equivalent to 1 : 1 (water : ChCl) mole ratio, a concentration that has previously[12] been observed to correspond to a transition in behaviour of other deep eutectic solvents.

Lastly, diffusion measurements for both reline and ethaline have shown that water has two diffusion co-efficients, over all water concentrations, in the presence and absence of Zn. This suggests that water exists in two different environments, with no, or slow, exchange between these environments. As we see this bi-exponential diffusion co-efficient for water, over all water concentrations, it is unlikely that these environments are associated with the water within the DES network and interstitial water, which has been observed at >6 wt% water (reline) and >8 wt% (ethaline). It is unclear what the origins are for the bi-exponential diffusion co-efficient of water, and further studies are required.

Conclusions

This paper has investigated the role of Zn and water on solvation, and dynamics, in reline and ethaline DES systems, using ^{1}H NMR spectroscopy, T_1 NMR relaxation times, NMR diffusion and 2D NOESY/EXSY spectroscopy. In ethaline, it is found that Zn promotes proton exchange between hydroxyl protons (H_d and H_f) in ChCl and EG, in the presence and absence of water. However, in reline, the presence of Zn was found to have little effect on the interactions between ChCl and U species, but did reduce the proton exchange between hydroxyl (H_d) and water (H_w) protons, in systems containing water. The presence of water was also found to change the interaction between ChCl and U species, removing the nOe cross-peak between amide and hydroxyl protons. These findings reveal key changes in solvation and dynamics, in both reline and ethaline, as a function of water and Zn concentration, proving insight into the role of solvation and dynamics in these electrolytes for a range of Zn electrochemical applications. These data support previous observations of changes in microstructure for both reline and ethaline, with increasing water content. Moreover, the variation in T_1 NMR relaxation times, for certain proton environments, in both DES, also demonstrates the potential for Zn electrochemical processes to be visualised by operando magnetic resonance imaging.[27,28]

Data availability

The data generated in this study are available at https://doi.org/10.25500/edata.bham.00000719.

Conflicts of interest

There are no conflicts to declare.

Acknowledgements

The authors thank the University of Birmingham and EPSRC (grant EP/K039245/1) for financial support. YAZ thanks the Saudi Arabian Ministry of Higher Education and the chemistry department in Imam Abdulrahman Bin Faisal University for their financial support.

References

1 F. I. Danilov, V. S. Protsenko, A. A. Kityk, D. A. Shaiderov, E. A. Vasil'eva, U. P. Kumar and C. J. Kennady, *Prot. Met. Phys. Chem.*, 2017, **53**, 1131–1138.

2 V. S. Protsenko, L. S. Bobrova, D. E. Golubtsov, S. A. Korniy and F. I. Danilov, *Russ. J. Appl. Chem.*, 2018, **91**, 1106–1111.
3 A. P. Abbott, J. C. Barron and K. S. Ryder, *Trans. Inst. Met. Finish.*, 2009, **87**, 201–207.
4 A. P. Abbott, K. J. McKenzie and K. S. Ryder, *Ionic Liquids IV*, American Chemical Society, 2007, vol. 975, ch. 13, pp. 186–197.
5 A. P. Abbott, G. Capper, K. J. McKenzie, A. Glidle and K. S. Ryder, *Phys. Chem. Chem. Phys.*, 2006, **8**, 4214–4221.
6 W. Kao-ian, R. Pornprasertsuk, P. Thamyongkit, T. Maiyalagan and S. Kheawhom, *J. Electrochem. Soc.*, 2019, **166**, A1063–A1069.
7 E. L. Smith, A. P. Abbott and K. S. Ryder, *Chem. Rev.*, 2014, **114**, 11060–11082.
8 Q. Zhang, K. De Oliveira Vigier, S. Royer and F. Jerome, *Chem. Soc. Rev.*, 2012, **41**, 7108–7146.
9 E. L. Smith, *Trans. Inst. Met. Finish.*, 2014, **91**, 241–248.
10 A. P. Abbott, K. El Ttaib, G. Frisch, K. J. McKenzie and K. S. Ryder, *Phys. Chem. Chem. Phys.*, 2009, **11**, 4269–4277.
11 A. H. Whitehead, M. Pölzler and B. Gollas, *J. Electrochem. Soc.*, 2010, **157**, D328–D334.
12 C. D'Agostino, L. F. Gladden, M. D. Mantle, A. P. Abbott, E. I. Ahmed, A. Y. M. Al-Murshedi and R. C. Harris, *Phys. Chem. Chem. Phys.*, 2015, **17**, 15297–15304.
13 B. B. Hansen, S. Spittle, B. Chen, D. Poe, Y. Zhang, J. M. Klein, A. Horton, L. Adhikari, T. Zelovich, B. W. Doherty, B. Gurkan, E. J. Maginn, A. Ragauskas, M. Dadmun, T. A. Zawodzinski, G. A. Baker, M. E. Tuckerman, R. F. Savinell and J. R. Sangoro, *Chem. Rev.*, 2021, **121**, 1232–1285.
14 A. P. Abbott, J. C. Barron, G. Frisch, K. S. Ryder and A. F. Silva, *Electrochim. Acta*, 2011, **56**, 5272–5279.
15 A. P. Abbott, J. C. Barron, G. Frisch, S. Gurman, K. S. Ryder and A. Fernando Silva, *Phys. Chem. Chem. Phys.*, 2011, **13**, 10224–10231.
16 X. Ge, C. Gu, X. Wang and J. Tu, *J. Mater. Chem. A*, 2017, **5**, 8209–8229.
17 A. T. Celebi, T. J. H. Vlugt and O. A. Moultos, *J. Phys. Chem. B*, 2019, **123**, 11014–11025.
18 T. Zhekenov, N. Toksanbayev, Z. Kazakbayeva, D. Shah and F. S. Mjalli, *Fluid Phase Equilib.*, 2017, **441**, 43–48.
19 C. Ma, A. Laaksonen, C. Liu, X. Lu and X. Ji, *Chem. Soc. Rev.*, 2018, **47**, 8685–8720.
20 J. R. Bezerra-Neto, N. G. Sousa, L. P. M. dos Santos, A. N. Correia and P. de Lima-Neto, *Phys. Chem. Chem. Phys.*, 2018, **20**, 9321–9327.
21 C. Du, B. Zhao, X.-B. Chen, N. Birbilis and H. Yang, *Sci. Rep.*, 2016, **6**, 1–14.
22 P. E. Valverde, T. A. Green and S. Roy, *J. Appl. Electrochem.*, 2020, **50**, 699–712.
23 O. S. Hammond, D. T. Bowron and K. J. Edler, *Angew. Chem., Int. Ed.*, 2017, **56**, 9782–9785.
24 E. Posada, N. López-Salas, R. J. Jiménez Riobóo, M. L. Ferrer, M. C. Gutiérrez and F. del Monte, *Phys. Chem. Chem. Phys.*, 2017, **19**, 17103–17110.
25 A. Pandey and S. Pandey, *J. Phys. Chem. B*, 2014, **118**, 14652–14661.
26 J. C. Barron, Doctor of Philosophy, University of Leicester, 2009.
27 A. J. Davenport, M. Forsyth and M. M. Britton, *Electrochem. Commun.*, 2010, **12**, 44–47.
28 M. M. Britton, P. M. Bayley, P. C. Howlett, A. J. Davenport and M. Forsyth, *J. Phys. Chem. Lett.*, 2013, **4**, 3019–3023.
29 I. R. Kleckner and M. P. Foster, *Biochim. Biophys. Acta*, 2011, **1814**, 942–968.
30 KaleidaGraph (Synergy, USA).
31 T. D. W. Claridge, *High-Resolution NMR Techniques in Organic Chemistry*, 2nd edn, Elsevier, Oxford, UK, 2009.
32 E. O. Stejskal and J. E. Tanner, *J. Chem. Phys.*, 1965, **42**, 288.
33 R. R. Gil and A. Navarro-Vázquez, *Modern NMR Approaches to the Structure Elucidation of Natural Products: Volume 2: Data Acquisition and Applications to Compound Classes*, The Royal Society of Chemistry, 2017, vol. 2, pp. 1–38.
34 R. Stefanovic, M. Ludwig, G. B. Webber, R. Atkin and A. J. Page, *Phys. Chem. Chem. Phys.*, 2017, **19**, 3297–3306.
35 C. R. Ashworth, R. P. Matthews, T. Welton and P. A. Hunt, *Phys. Chem. Chem. Phys.*, 2016, **18**, 18145–18160.
36 N. Bloembergen, E. M. Purcell and R. V. Pound, *Phys. Rev.*, 1948, **73**, 679–712.

